Inorganic Chemistry

Article

pubs.acs.org/IC

Heterobimetallic Coordination Polymers Based on the $[Pt(SCN)_4]^{2-}$ and $[Pt(SeCN)_4]^{2-}$ Building Blocks

Masayuki Kobayashi,[†,‡] Didier Savard,[†] Andrew R. Geisheimer,[†] Ken Sakai,*[,‡] and Daniel B. Leznoff*[,†]

[†]Department of Chemistry, Simon Fraser University, 8888 University Drive, Burnaby, British Columbia, V5A 1S6, Canada

[‡]Department of Chemistry, Faculty of Science, Kyushu University, Hakozaki 6-10-1, Higashi-ku, Fukuoka, 812-8581, Japan

Supporting Information

ABSTRACT: New complexes and the first coordination polymers containing $[Pt(SCN)_4]^{2-}$ of the type $[M(L)_x][Pt(SCN)_4]$ (where L = 2,2′-bipyridine (bipy), x = 2, M = Co(II), Ni(II), Cu(II); L = ethylenediamine (en), x = 2, M = Ni(II), Cu(II); L = *N*,*N*,*N*′,*N*′-tetramethylethylenediamine (tmeda), x = 1, M = Cu(II); L = 2,2′;6′,2″-terpyridine (terpy), x = 1, M = Mn(II), Co(II); L = 1,10-phenanthroline (phen), x = 2, M = Pb(II)) were prepared by reacting the appropriate metal–ligand cations with $K_2[Pt(SCN)_4]$ and structurally characterized. $[M(bipy)_2Pt(SCN)_4]_2 \cdot 2MeOH$ (M = Co (**1**), Cu (**4**)) consist of supramolecular tetranuclear distorted squares containing two $[M(bipy)_2]^{2+}$ and two $[Pt(SCN)_4]^{2+}$ units. $[Cu(bipy)_2(NCS)]_2[Pt(SCN)_4]$ (**6**) is a double salt of the $[Pt(SCN)_4]^{2-}$ anion and two $[Cu(bipy)(NCS)]^+$ cations. $[Cu(en)_2Pt(SCN)_4]$ (**7**, **8**) are 1-D coordination polymers that are coordinated in either cis or trans fashion at the $[Pt(SCN)_4]^{2-}$ unit, for **7** and **8**, respectively. Complexes $[Cu(en)_2Pt(SeCN)_4]$ (**9**) and $[Ni(en)_2Pt(SCN)_4]$ (**10**) are similar to **8** and **7**, respectively, but complex **9** (prepared using $(^nBu_4N)_2[Pt(SeCN)_4]$) also presents intermolecular Se–Se interactions which resulted in an increased dimensionality. Compounds $[M(terpy)Pt(SCN)_4]$ (M = Mn (**11**), Co (**13**)) involve 2-D sheets of $[M(terpy)]^{2+}$ and $[Pt(SCN)_4]^{2-}$ units, whereas $[Mn(terpy)_2][Pt(SCN)_4]$ (**12**) is a double salt of one $[Mn(terpy)_2]^{2+}$ unit and one $[Pt(SCN)_4]^{2-}$. $[Cu(tmeda)Pt(SCN)_4]$ (**14**) contains a five-coordinate Cu^{2+} metal center coordinated to one tmeda ligand and three different $[Pt(SCN)_4]^{2-}$ units, resulting in 2-D sheets. $[Pb(phen)_2Pt(SCN)_4]$ (**15**) contains an 8-coordinate Pb^{2+} metal center coordinated to two phen ligands and four $[Pt(SCN)_4]^{2-}$, generating a 3-D network in the solid state. Structural correlations were established between the ancillary ligand, the choice of metal, the structure of the $[Pt(SCN)_4]^{2-}$ building block, and the resulting dimensionality of the coordination polymers.

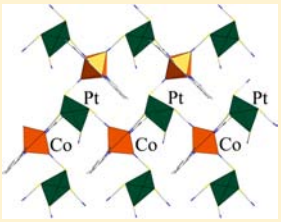

INTRODUCTION

Self-assembly of coordination polymers using organic and/or metal-based ancillary ligands and metal cation nodes is an effective route for synthesis of hybrid organic/inorganic materials with tunable physical and chemical properties.[1−5] In order to generate materials in a rational fashion, attaining control over the geometric preferences and overall structural dimensionality of coordination polymers is a critical goal.[6−8] The characteristics of both the capping ancillary ligands and the inorganic building blocks are central to achieving such control over the structure of the final self-assembled product. These characteristics include, but are not limited to, available coordination sites, coordination geometry preference, ligand flexibility, ligand bulkiness, and hydrogen bond interactions.[9−17]

Prussian Blue analogues, which are cyanometallate building block-based coordination polymers, are an archetypical example of coordination polymer synthesis with definitive control over structural features and physical/chemical properties.[18−29] Use of octahedral metal cations and octahedral cyanometallate anions yields the well-known bimetallic, cubic 3-D array in which the choice of metal(s) does not significantly impact the structure; this control has permitted rational tuning of the magnetic properties of Prussian Blue analogues, including ferro- and ferrimagnetic ordering temperatures and photomagnetic effects, for example. Similarly, square-planar cyanometallate building blocks of the type $[M(CN)_4]^{2-}$ (M = Ni, Pd, Pt) are known to generate 2-D sheet structures, which can be interlinked by addition of other neutral bridging ligands.[30−39] In particular, the d^8 $[Pt(CN)_4]^{2-}$ unit has been used extensively in coordination polymer synthesis, since it is very stable, kinetically inert, and known to form metallophilic d^8–d^8 and d^8–d^{10} interactions that serve to increase structural dimensionality and also induce a range of useful physical and chemical properties, including vapochromism, luminescence, and conductivity (when doped).[40−60]

On the other hand, the d^8 thiocyanate analogue $[Pt(SCN)_4]^{2-}$ and its heavier congener $[Pt(SeCN)_4]^{2-}$ have been virtually unexplored as building blocks for coordination polymers; the only reported heterometallic system is the trinuclear $\{Pt(SCN)_2[(\mu\text{-}SCN)Mn(NCS)(bipy)_2]_2\}$ complex,[61] which is luminescent at low temperatures. To our knowledge, there are no structurally characterized coordination polymers with these units. Thus, we posed the following questions: Can coordination polymers be prepared with $[Pt(SCN)_4]^{2-}$, and what kind of structural/physical properties can be accessed? Critically, do metallophilic Pt–Pt bonding or

Received: October 29, 2012
Published: April 11, 2013

 © 2013 American Chemical Society dx.doi.org/10.1021/ic302360b | *Inorg. Chem.* 2013, 52, 4842−4852

other secondary interactions play a role in the structural dimensionality and supramolecular architectures of the resulting materials? The $[Pt(SCN)_4]^{2-}$ anion is comparable to $[Pt(CN)_4]^{2-}$ in the sense that it can bridge up to four metal centers via the four thiocyanate species and thus increase the dimensionality of the resulting coordination polymer. However, the SCN^- unit coordinates at an angle of approximately 50−70° to the Pt(II) center, as opposed to the strictly linear coordination for the analogous CN^- species.[62−73]

In order to explore these questions in a systematic fashion, we targeted a variety of M(II) cations (M = Mn, Co, Ni, Cu, and Pb) and a prescribed set of ancillary capping ligands (L = 2,2′-bipyridine (bipy), 1,2-ethylenediamine (en), *N*,*N*,*N*′,*N*′-tetramethylethylenediamine (tmeda), 2,2′;6′,2″-terpyridine (terpy), and 1,10-phenanthroline (phen)) to react with $[Pt(SCN)_4]^{2-}$ (and in one case $[Pt(SeCN)_4]^{2-}$) units. Thus, herein we present the synthesis and structure of the resulting coordination polymers of the type $[M(L)_x][Pt(SCN)_4]$ (where L = 2,2′-bipy, x = 2, M = Co(II), Ni(II), Cu(II); L = en, x = 2, M = Ni(II), Cu(II); L = tmeda, x = 1, M = Cu(II); L = terpy, x = 1, M = Mn(II), Co(II); L = phen, x = 2, M = Pb(II)) and examine the factors influencing the dimensionality of the product materials, including the choice of metal ion, ancillary capping ligand, and bridging nature of the $[Pt(SCN)_4]^{2-}$ building block. To our knowledge, these materials represent the first coordination polymers using the $[Pt(XCN)_4]^{2-}$ (X = S, Se) building blocks.

EXPERIMENTAL SECTION

General Procedures and Physical Measurements. All manipulations were performed in air using purified solvents. K_2PtCl_4 was purchased from Tanaka Kikinzoku Kogyo and used as received. $(^nBu_4N)_2[Pt(SeCN)_4]$ was synthesized as previously described.[74] All other reagents were obtained from commercial sources and used as received. IR spectra were obtained using a Perkin-Elmer Spectrum One FT-IR with an ATR attachment or a Thermo Nicolet 670 FT-IR spectrometer using KBr pellets. Raman Spectra were recorded on a Renishaw inVia Raman Microscope equipped with a 200 mW 785 nm laser. Spectra were obtained from 100 to 4000 cm^{-1} using a 1200 l/mm (633/780) grating for an exposure time of 10 s. Specific accumulations (a) and laser power (% lp) are stated for each experiment. Microanalyses (C, H, N) were performed at Simon Fraser University using a computer-controlled Carlo Erba (Model 1106) CHN analyzer or at Kyushu University using a Yanako CHN recorder MT-5 or MT-6. Powder X-ray diffractograms were obtained using a Bruker D8 ADVANCE equipped with a Cu Kα source (λ = 1.54056 Å) or using a Bruker SMART diffractometer equipped with an APEX II CCD detector and a IμCu Kα microfocus sealed X-ray tube (λ = 1.54056 nm) fitted with HELIOS multilayer optics. Magnetic susceptibility data were collected using a Quantum Design MPMS Evercool XL-7 between 1.8 and 300 K with a 1000 Oe field strength. Samples were measured in low background gel caps and straws. Data was corrected for TIP and the constituent atoms by use of Pascal constants.[75]

Synthetic Procedures. *CAUTION: Although we experienced no difficulties, perchlorate salts are potentially explosive and should only be used in small quantities and handled with care.*

$K_2[Pt(SCN)_4]$. $K_2[Pt(SCN)_4]$ was synthesized by modification of a literature procedure.[76] To 10 mL of an aqueous solution of $K_2[PtCl_4]$ (1.03 g, 2.50 mmol) was added 10 mL of an aqueous solution of KSCN (0.972 g, 10.0 mmol). The solution was heated at 60 °C for 15 min, and the volume of the solution was reduced to approximately 5 mL by heating over a steam bath. Then 20 mL of acetone was added to the mixture, and the white precipitate of KCl was filtered. The solvent was removed using a rotary evaporator, and the crude residue was dissolved in a minimum amount of ethyl acetate. The white precipitate of KSCN was filtered, and the solvent was removed using a rotary evaporator. The resulting crude residue of $K_2[Pt(SCN)_4]$ was recrystallized from acetone by slow evaporation. Yield: 1.24 g (97.8%). FT-IR (ATR, cm^{-1}): 3433, 2795, 2124 (ν_{CN}), 2097 (ν_{CN}), 2047 (ν_{CN}), 1624, 1111, 967, 957, 749, 484. Raman (785 nm; a, 1; % lp, 50, cm^{-1}): 2128 (ν_{CN}), 2102 (ν_{CN}), 700, 464, 309, 293, 174, 142, 122. Spectroscopic data is consistent with reported literature values.[76]

$[Co(bipy)_2Pt(SCN)_4]_2\cdot 2MeOH$ (1) and $[Co(bipy)_2][Pt(SCN)_4]\cdot H_2O$ (2). To 2 mL of an aqueous solution of $Co(NO_3)_2\cdot 6H_2O$ (0.029 g, 0.10 mmol) was added 2 mL of a methanolic solution of 2,2′-bipyridine (0.031 g, 0.20 mmol). Then, 4 mL of an aqueous solution of $K_2[Pt(SCN)_4]$ (0.051 g, 0.10 mmol) was added dropwise to this yellow solution. An immediate orange precipitate of $[Co(bipy)_2][Pt(SCN)_4]\cdot H_2O$ (**2**) formed, which was collected by filtration and dried in vacuo. Yield: 0.080 g (97%). Anal. Calcd for $C_{24}H_{18}N_8CoOPtS_4$: C, 35.29; H, 2.22; N,13.72. Found: C, 35.22; H, 2.23; N, 13.67. FT-IR (ATR, cm^{-1}): 3449, 2146 (ν_{CN}), 2119 (ν_{CN}), 1597, 1575, 1491, 1472, 1441, 1314, 1248, 1155, 1102, 1060, 1021, 761, 735, 651, 632, 432, 410. By slow diffusion in a vial of a methanolic solution of $K_2[Pt(SCN)_4]$, into a 1:1 H_2O/methanol mixture solution of Co/bipy at room temperature, after several days, orange plates of $[Co(bipy)_2Pt(SCN)_4]_2\cdot 2MeOH$ (**1**) were obtained. Anal. Calcd for $C_{48}H_{32}Co_2N_{16}Pt_2S_8\cdot 2CH_3OH$: C, 36.14; H, 2.43; N, 13.49. Found: C, 35.66; H, 2.44; N, 13.57. IR (ATR, cm^{-1}): 3443, 3112, 3073, 2934, 2815, 2144 (ν_{CN}), 2130 (ν_{CN}), 2116 (ν_{CN}), 1596, 1574, 1565, 1490, 1471, 1439, 1312, 1247, 1154, 1101, 1073, 1059, 1020, 808, 760, 734, 651, 631, 470, 431, 415, 406. $\chi_M T$ (300 K, 1000 Oe) = 3.25 cm^3 K mol^{-1}. The powder X-ray diffractogram of **2** is completely different than that of **1** (Figure S3, Supporting Information).

$[Ni(bipy)_2][Pt(SCN)_4]$ (3). To 2 mL of an aqueous solution of $Ni(NO_3)_2\cdot 6H_2O$ (0.029 g, 0.10 mmol) was added 2 mL of a methanolic solution of 2,2′-bipyridine (0.031 g, 0.20 mmol). Then, 4 mL of an aqueous solution of $K_2[Pt(SCN)_4]$ (0.051 g, 0.10 mmol) was added dropwise to this pale red solution. An immediate pale yellow precipitate of $[Ni(bipy)_2][Pt(SCN)_4]$ (**3**) formed, which was collected by filtration and dried in vacuo. Yield: 0.075 g (94%). Anal. Calcd for $C_{24}H_{16}N_8NiPtS_4$: C, 36.10; H, 2.02; N, 14.03. Found: C, 36.44; H, 2.05; N, 13.99. FT-IR (ATR, cm^{-1}): 3465, 3078, 2143 (ν_{CN}), 2112 (ν_{CN}), 1599, 1576, 1568, 1492, 1472, 1442, 1314, 1281, 1248, 1221, 1172, 1157, 1105, 1061, 1044, 1022, 967, 893, 835, 809, 760, 735, 692, 653, 634, 549, 471, 441, 416. The powder was nearly amorphous by X-ray diffraction.

$[Cu(bipy)_2Pt(SCN)_4]_2\cdot 2MeOH$ (4), $[Cu(bipy)_2][Pt(SCN)_4]$ (5), and $[Cu(bipy)_2(NCS)]_2[Pt(SCN)_4]$ (6). To 2 mL of an aqueous solution of $Cu(ClO_4)_2\cdot 6H_2O$ (0.037 g, 0.099 mmol) was added 2 mL of a methanolic solution of 2,2′-bipyridine (0.031 g, 0.20 mmol). Then, 4 mL of an aqueous solution of $K_2[Pt(SCN)_4]$ (0.051 g, 0.10 mmol) was added dropwise to this blue solution. An immediate green precipitate of $[Cu(bipy)_2][Pt(SCN)_4]$ (**5**) formed, which was collected by filtration and dried in vacuo. The powder was nearly amorphous by X-ray diffraction. Yield: 0.068 g (85%). Anal. Calcd for $C_{24}H_{16}N_8CuPtS_4$: C, 35.88; H, 2.01; N, 13.95. Found: C, 35.50; H, 1.97; N, 13.71. FT-IR (ATR, cm^{-1}): 3076, 2107 (ν_{CN}), 1600, 1567, 1494, 1472, 1442, 1314, 1249, 1156, 1102, 1061, 1044, 1029, 1014, 760, 729, 660, 636, 650, 464, 407. $\chi_M T$ (300 K, 1000 Oe) = 0.39 cm^3 K mol^{-1}. By slow diffusion in a vial of a methanolic solution of a Cu/bipy mixture into a methanolic solution of $K_2[Pt(SCN)_4]$ at 5 °C after several days green plates of $[Cu(bipy)_2Pt(SCN)_4]_2\cdot 2MeOH$ (**4**) were obtained. Anal. Calcd for $C_{50}H_{40}N_{16}Cu_2Pt_2O_2S_8$: C, 35.94; H, 2.41; N, 13.41. Found: C, 35.66; H, 2.35; N, 13.52. FT-IR (ATR, cm^{-1}): 3549, 3061, 2140 (ν_{CN}), 2112 (ν_{CN}), 1602, 1595, 1575, 1567, 1494, 1472, 1441, 1314, 1279, 1250, 1171, 1156, 1120, 1104, 1072, 1056, 1044, 1010, 974, 907, 892, 808, 761, 730, 694, 650, 632, 441, 431, 405. $\chi_M T$ (300 K, 1000 Oe) = 0.40 cm^3 K mol^{-1}. Green prisms of $[Cu(bipy)_2(NCS)]_2[Pt(SCN)_4]$ (**6**) were obtained by slow diffusion in a vial of a methanolic solution of a Cu/bipy mixture into an aqueous solution of $K_2[Pt(SCN)_4]$ at 5 °C. Anal. Calcd for $C_{46}H_{32}N_{14}S_6Cu_2Pt$: C, 42.65; H, 2.49; N, 15.14. Found: C, 42.39; H, 2.58; N, 15.11. FT-IR (ATR, cm^{-1}): 3074, 3031, 2114 (ν_{CN}), 2101 (ν_{CN}), 2063 (ν_{CN}), 1600, 1566, 1495, 1473, 1443, 1315, 1250, 1177, 1156, 1103, 1061, 1045,

dx.doi.org/10.1021/ic302360b | *Inorg. Chem.* 2013, 52, 4842−4852

1029, 1013, 971, 910, 849, 812, 772, 765, 730, 692, 659, 649, 635, 467, 439, 418, 404.

[Cu(en)$_2$Pt(SCN)$_4$] (cis, 7; trans, 8). To 4 mL of an aqueous solution of Cu(NO$_3$)$_2$·3H$_2$O (0.025 g, 0.10 mmol) was added 2 mL of a stock methanolic solution (0.1 M) of ethylenediamine (en). Then, 6 mL of a methanol/water (1:2) solution of K$_2$[Pt(SCN)$_4$] (0.051 g, 0.10 mmol) was added dropwise to this purple solution. An immediate brown precipitate of *cis*-[Cu(en)$_2$Pt(SCN)$_4$] (**7**) formed, which was collected by filtration and dried in vacuo. Yield: 0.037 g (59%). Anal. Calcd for C$_8$H$_{16}$N$_8$CuPtS$_4$: C, 15.72; H, 2.64; N, 18.33. Found: C, 15.59; H, 2.48; N, 18.17. FT-IR (ATR, cm^{-1}): 3305, 3253, 3156, 2942, 2883, 2126 (ν_{CN}), 2108 (ν_{CN}), 1581, 1456, 1394, 1369, 1321, 1276, 1157, 1090, 1026, 968, 878, 698, 529, 459, 432, 420. $\chi_M T$ (300 K, 1000 Oe) = 0.39 cm^3 K mol^{-1}. To obtain X-ray-quality crystals the "Petri dish diffusion method" was used, in which a Petri dish containing an aqueous solution of Cu(ClO$_4$)$_2$·6H$_2$O and 2 equiv of en on one side and an aqueous solution of K$_2$[Pt(SCN)$_4$] on the other side was prepared. Slow diffusion of the two reagents yielded brown crystals of **7** over several days. The simulated powder X-ray diffraction (PXRD) pattern from this crystal after structure solution was comparable to the PXRD pattern of the initial powder (Supporting Information, Figure S4).

However, by layering a solution of Cu(ClO$_4$)$_2$·6H$_2$O and 2 equiv of en in methanol onto a solution of K$_2$[Pt(SCN)$_4$] in methanol and storing this in a sealed vial at 5 °C for several days, a mixture of brown crystals of **7** and purple crystals of *trans*-[Cu(en)$_2$Pt(SCN)$_4$] (**8**) was obtained, which were separated by hand. Anal. Calcd for C$_8$H$_{16}$N$_8$CuPtS$_4$ (**8**): C, 15.72; H, 2.64; N, 18.33. Found: C, 15.89; H, 2.57; N, 18.33. FT-IR (ATR, cm^{-1}): 3318, 3264, 2978, 2941, 2883, 2811, 2122 (ν_{CN}), 2103 (ν_{CN}), 1606, 1572, 1457, 1364, 1312, 1276, 1252, 1142, 1078, 1028, 1012, 961, 876, 860, 692, 603, 530, 469, 428, 421, 407.

[Cu(en)$_2$Pt(SeCN)$_4$] (9). To 18 mL of a methanolic solution of Cu(NO$_3$)$_2$·3H$_2$O (0.025 g, 0.10 mmol) was added 2 mL of a stock methanolic solution (0.1 M) of ethylenediamine. Then this solution was added dropwise to 30 mL of a methanol/ethanol (1:2) solution of (Bu$_4$N)$_2$[Pt(SeCN)$_4$] (0.11 g, 0.10 mmol). Overnight, crystals of [Cu(en)$_2$Pt(SeCN)$_4$] (**9**) grew, which were then collected by filtration and dried in air. Yield: 0.063 g (78%). Anal. Calcd for C$_8$H$_{16}$N$_8$CuPtSe$_4$: C, 12.03; H, 2.02; N, 14.03. Found: C, 12.16; H, 2.01; N, 14.03. FT-IR (ATR, cm^{-1}): 3307, 3246, 2120 (ν_{CN}), 2103 (ν_{CN}), 1575, 1455, 1365, 1275, 1154, 1084, 1031, 963, 694, 532, 473, 413. $\chi_M T$ (300 K, 1000 Oe) = 0.38 cm^3 K mol^{-1}.

[Ni(en)$_2$Pt(SCN)$_4$] (10). Ni(NO$_3$)$_2$·6H$_2$O (0.029 g, 0.10 mmol) was added to 5 mL of an aqueous stock solution (0.04 M) of ethylenediamine. Then, 5 mL of an aqueous solution of K$_2$[Pt(SCN)$_4$] (0.051 g, 0.10 mmol) was added dropwise to this pale purple solution. An immediate orange precipitate of [Ni(en)$_2$Pt(SCN)$_4$] (**10**) formed, collected by filtration, and dried in vacuo. Yield: 0.058 g (96%). Anal. Calcd for C$_8$H$_{16}$N$_8$NiPtS$_4$: C, 15.85; H, 2.66; N, 18.48. Found: C, 15.75; H, 2.59; N, 18.38. FT-IR (ATR, cm^{-1}): 3331, 3278, 2944, 2878, 2140 (ν_{CN}), 2110 (ν_{CN}), 1581, 1456, 1324, 1275, 1146, 1087, 1024, 1004, 960, 872, 667, 515, 427. $\chi_M T$ (300 K, 1000 Oe) = 1.19 cm^3 K mol^{-1}. To obtain the X-ray-quality crystals of **10**, a Petri dish was divided with a filter paper. A 1 mL amount of a 20 mM aqueous solution of [Ni(en)$_2$](NO$_3$)$_2$ was prepared on one side, and 1 mL of a 20 mM aqueous solution of K$_2$[Pt(SCN)$_4$] was inserted on the other side.[77] The two solutions diffused slowly into each other. Several days later, yellow plate-like crystals of X-ray quality were obtained. IR and PXRD data of the crystals matched that of powdered **10** (Supporting Information, Figure S5).

[Mn(terpy)Pt(SCN)$_4$] (11) and [Mn(terpy)$_2$][Pt(SCN)$_4$] (12). To 5 mL of an aqueous solution of MnCl$_2$·4H$_2$O (0.020 g, 0.10 mmol) was added 5 mL of a methanolic solution of terpyridine (terpy; 0.022 g, 0.094 mmol). Then, 10 mL of a methanolic solution of K$_2$[Pt(SCN)$_4$] (0.050 g, 0.10 mmol) was diffused slowly into this solution by layering or slow diffusion through a filter paper. Yellow plate-like crystals of [Mn(terpy)Pt(SCN)$_4$] (**11**) were obtained in low yield after several days at 5 °C. Yield: 0.019 g (26%). Anal. Calcd for C$_{19}$H$_{11}$N$_7$MnPtS$_4$: C, 31.89; H, 1.55; N, 13.70. Found: C, 31.91; H, 1.70; N, 13.44. FT-IR (ATR, cm^{-1}): 2119 (ν_{CN}), 1592, 1571, 1474, 1459, 1448, 1438, 1402, 1312, 1247, 1186, 1168, 1159, 1094, 1014, 768, 658, 651, 639, 512, 425. Attempts to make **11** in powder form by mixing the reagents in a range of solvents (water, methanol, ethanol etc.) resulted in a yellow powder. Crystals of [Mn(terpy)$_2$][Pt(SCN)$_4$] (**12**) were grown from the filtered mixtures after several days at 5−8 °C or from the reaction mixture of **11** after disturbance of the layers. PXRD patterns measured for the powders resulting from direct mixing of the reagents were the same as the PXRD pattern generated from the crystals of **12** (Supporting Information, Figure S6). Yield: 0.085 g (89%). Anal. Calcd for C$_{34}$H$_{22}$N$_{10}$MnPtS$_4$: C, 43.03; H, 2.33; N, 14.76. Found: C, 42.74; H, 2.28; N, 14.91. FT-IR (ATR, cm^{-1}): 2107 (ν_{CN}), 1594, 1572, 1476, 1459, 1451, 1438, 1312, 1290, 1245, 1191, 1166, 1159, 1013, 769.

[Co(terpy)Pt(SCN)$_4$] (13) and [Co(terpy)$_2$][Pt(SCN)$_4$] (13b). To 5 mL of an aqueous solution of Co(NO$_3$)$_2$·6H$_2$O (0.030 g, 0.10 mmol) was added 5 mL of a methanolic solution of terpyridine (0.023 g, 0.099 mmol). Then, the resulting mixture was layered over 10 mL of an aqueous solution of K$_2$[Pt(SCN)$_4$] (0.050 g, 0.10 mmol). After 24 h, a cocrystallized 65:35 mixture of red plates (**13**) and red blocks (**13b**) was obtained. Direct mixing of the reagents resulted in an orange powder that consists of **13** and **13b** in a similar ratio. Yield (mixture): 0.045 g (62%). Anal. Calcd for 65:35 powder mixture of C$_{19}$H$_{11}$N$_7$CoPtS$_4$: C$_{34}$H$_{22}$N$_{10}$CoPtS$_4$: C, 36.36; H, 1.87; N, 14.07. Found: C, 36.78; H, 1.73; N, 13.64. Anal. Calcd for 65:35 crystals mixture of C$_{19}$H$_{11}$N$_7$CoPtS$_4$: C$_{34}$H$_{22}$N$_{10}$CoPtS$_4$: C, 36.36; H, 1.87; N, 14.07. Found: C, 36.47; H, 1.70; N, 13.76. FT-IR (powder mixture, ATR, cm^{-1}): 2135 (ν_{CN}), 2112 (ν_{CN}), 1598, 1571, 1467, 1444, 1396, 1249, 1160, 1016, 770, 769. FT-IR (**13**, ATR, cm^{-1}): 2135 (ν_{CN}), 1597, 1570, 1465, 1444, 1396, 1283, 1242, 1186, 1155, 1013, 769, 648, 515, 456, 426, 417. FT-IR (**13b**, KBr, cm^{-1}): 2113 (ν_{CN}), 1597, 1570, 1465, 1444, 1396, 1286, 1242, 1186, 1153, 1054, 1013, 770.

[Cu(tmeda)Pt(SCN)$_4$] (14). Cu(ClO$_4$)$_2$·6H$_2$O (0.037 g, 0.10 mmol) was added to 5 mL of an aqueous stock solution (0.02 M) of *N*,*N*,*N*′,*N*′-tetramethylethylenediamine (tmeda). Then, 5 mL of an aqueous solution of K$_2$[Pt(SCN)$_4$] (0.051 g, 0.10 mmol) was added dropwise to this blue solution. An immediate green precipitate of [Cu(tmeda)Pt(SCN)$_4$] (**14**) formed, which was collected by filtration and dried in vacuo. Yield: 0.056 g (91%). Anal. Calcd for C$_{10}$H$_{16}$N$_6$CuPtS$_4$: C, 19.78; H, 2.66; N, 13.84. Found: C, 19.77; H, 2.56; N, 13.94. FT-IR (ATR, cm^{-1}): 2908, 2158 (ν_{CN}), 2134 (ν_{CN}), 2117 (ν_{CN}), 2091 (ν_{CN}), 1464, 1390, 1286, 1244, 1128, 1051, 1018, 1001, 952, 812, 770, 598, 513, 468, 443. $\chi_M T$ (300 K, 1000 Oe) = 0.41 cm^3 K mol^{-1}. To obtain X-ray-quality crystals, a Petri dish containing a methanol solution of Cu(ClO$_4$)$_2$·6H$_2$O and a stoichiometric amount of tmeda on one side and a methanol solution of K$_2$[Pt(SCN)$_4$] on the other side was prepared. Slow diffusion of the two reagents yielded green crystals of **14** over several days. The crystals had comparable IR and PXRD data (Supporting Information, Figure S7) to the powder.

[Pb(phen)$_2$Pt(SCN)$_4$] (15). Pb(NO$_3$)$_2$ (0.034 g, 0.10 mmol) was dissolved in 15 mL of a solution of water and methanol (1:1). To the mixture was added 15 mL of a solution of 1,10-phenanthroline·H$_2$O (0.040 g, 0.20 mmol) in water and methanol (1:1). The resulting solution was stirred for 15 min. Then, a water/methanol (1:1) solution (8 mL) of K$_2$[Pt(SCN)$_4$] (0.051 g, 0.10 mmol) was added dropwise while stirring. The precipitated orange powder was collected by filtration and dried under vacuum. Yield: 0.086 g (85%). Anal. Calcd for C$_{28}$H$_{16}$N$_8$PbPtS$_4$: C, 33.80; H, 1.62; N, 11.26. Found: C, 33.54; H, 1.62; N, 11.30. FT-IR (powder, ATR, cm^{-1}): 2105 (ν_{CN}), 1626, 1590, 1518, 1513, 1497, 1426, 1340, 1219, 1140, 1098, 860, 846, 838, 764, 726, 718.

To obtain single crystals of **15**, 5 mL of a 4 mM methanolic solution of K$_2$[Pt(SCN)$_4$] was mixed gently with 5 mL of a 4 mM solution of [Pb(phen)$_2$](NO$_3$)$_2$ in water and methanol (1:1). The mixture was filtered and left undisturbed at 5 °C for recrystallization over a period of a few days, which yielded yellow crystals. FT-IR (crystals, ATR, cm^{-1}): 2103 (ν_{CN}), 1622, 1589, 1572, 1513, 1495, 1423, 1342, 1300, 1219, 1204, 1141, 1099, 1034, 969, 956, 860, 843, 767, 725, 719, 635, 469, 427, 414. Although the IR data of the powder and crystals are very similar, the powder X-ray diffractogram (Figure S8, Supporting

dx.doi.org/10.1021/ic302360b | Inorg. Chem. 2013, 52, 4842−4852

Information) of the powder indicates a mixture of **15** as the minor product and another material (likely a polymorph of **15**) as the major product.

Single-Crystal X-ray Diffraction Analyses. All crystals were mounted on glass fibers using epoxy adhesive or using a Mitegen Cryoloop cryogenic sample holder with *n*-paratone. Data sets were collected using a Bruker Smart APEX II instrument at 100 K, except for **12** which was collected at 293 K. The temperature was regulated using an Oxford Cryosystems Cryostream. Data reduction for all compounds included corrections for Lorentz and polarization effects. Empirical absorption corrections were applied to all data sets (SADABS1). Initial structure solutions were obtained by direct methods, and SHELXL-972 was used to refine the atomic parameters.[104]

For all compounds, coordinates and anisotropic displacement parameters for the non-hydrogen atoms were refined; for compound **14**, disorder in the tmeda ligand was modeled appropriately and the resulting partial occupancy atoms were refined using isothermal parameters. For all compounds, hydrogen atoms were placed in calculated positions (methylene and aromatic C−H at d = 0.97 and 0.93 Å; d N−H = 0.93 Å) and their coordinate shifts were linked with those of the respective carbon or nitrogen atoms during refinement. Isotropic thermal parameters for the hydrogen atoms were initially assigned proportionately to the equivalent isotropic thermal parameters of their respective carbon or nitrogen atoms. Subsequently, isotropic thermal parameters for C−H hydrogen atoms were constrained to have identical shifts during refinement, as were those N−H hydrogen atoms. Crystallographic data for all complexes are available in the Supporting Information as Tables S1 (**1**, **4**, **6**, **7**), S2 (**8**−**11**), and S3 (**12**−**15**), with further refinement details available in cif format for all structures. Tables of bond lengths and angles are also available in the Supporting Information.

RESULTS

Infrared Spectroscopy. IR spectra of all complexes clearly show the presence of the SCN^- groups, with their ν_{CN} bands ranging from 2101 (**6**) to 2146 cm^{-1} (**2**). These bands are shifted from the ν_{CN} absorbances of 2124, 2097, and 2047 cm^{-1} for $K_2[Pt(SCN)_4]$, suggesting the presence of a combination of both bridging and nonbridging SCN^- groups (depending on the product), given that the IR bands of bridging thiocyanates shift to higher energy values, as observed for cyanide bridging moieties.[78]

Synthesis and Structural Studies of $[M(bipy)_2][Pt(SCN)_4]$ (M = Co, Ni, Cu). Addition of $K_2[Pt(SCN)_4]$ to $[M(bipy)_2]X_2$ (M = Co(II), Ni(II), Cu(II); X = ClO_4 or NO_3 as per the Experimental Section) yielded a series of heterobimetallic complexes with different solvates. For example, when aqueous/methanol solutions of CoX_2 and $K_2[Pt(SCN)_4]$ were mixed quickly, the aqueous solvate powder $[Co(bipy)_2][Pt(SCN)_4]\cdot H_2O$ (**2**) precipitated out of solution immediately. However, when mixing the compounds by slow diffusion, the tetranuclear complex $[Co(bipy)_2Pt(SCN)_4]_2\cdot 2MeOH$ (**1**) was obtained instead as single crystals. Changing the metal-to-ligand ratio did not result in preferential formation of **1** or any other compound. In addition, changing the solvent mixture generally resulted in precipitation of the powder **2** only, which was shown to have a different (but undetermined) structure than **1** by powder X-ray diffraction (Figure S3, Supporting Information). In the case of Ni(II), only an amorphous powder with composition $[Ni(bipy)_2][Pt(SCN)_4]$ (**3**) could be obtained even by slow diffusion or changing the solvent composition.

In the case of Cu(II), using the same reaction conditions as for **2** yielded an amorphous powder with composition $[Cu(bipy)_2][Pt(SCN)_4]$ (**5**). However, two different complexes were obtained by slow diffusion of the same reagents. Using methanol only as a solvent resulted in tetranuclear complex $[Cu(bipy)_2Pt(SCN)_4]_2\cdot 2MeOH$ (**4**), while decomposition product $[Cu(bipy)_2(NCS)]_2[Pt(SCN)_4]$ (**6**) was formed at the water/methanol interface when the two solvents were used in the diffusion crystallization.

Structural studies of **1** (Figure 1) revealed that the complex consists of a zero-dimensional (0-D) tetranuclear distorted

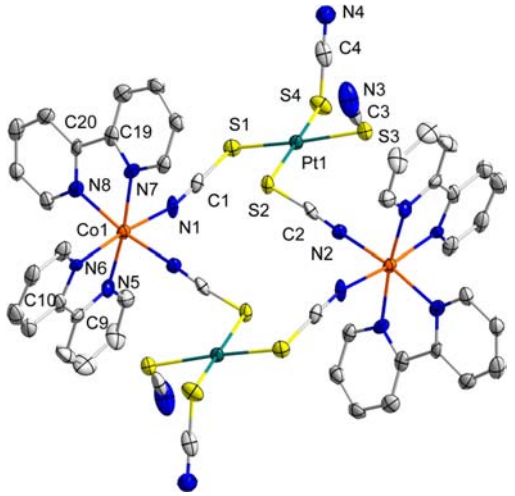

Figure 1. Molecular structure of $[Co(bipy)_2Pt(SCN)_4]_2\cdot 2MeOH$ (**1**). Hydrogen atoms and methanol solvate have been omitted for clarity. Thermal ellipsoids are drawn at 50% probability. Color code: orange (Co), green (Pt), blue (N), gray (C), yellow (S). Selected bond lengths (Å): Co−N1 = 2.131(8), Co−N2′ = 2.095(8), Co1−N5 = 2.09(1), Co1−N6 = 2.124(8), Co1−N7 = 2.133(9), Co1−N8 = 2.144(8).

supramolecular square composed of two $[Co(bipy)_2]^{2+}$ and two $[Pt(SCN)_4]^{2-}$ units. Each Co(II) center is coordinated to two 2,2′-bipyridine ligands in a cis fashion, occupying four coordination sites. The two remaining coordination sites are occupied by N-bound SCN^- bridges to the Pt(II) metal centers, leading to a six-coordinate octahedral Co(II) geometry. Thus, the choice and orientation of the ancillary bipy ligands on the Co(II) center generates what can be termed a "cis-4 + 2" nodal site: a metal center with 4 blocked coordination sites and two cis sites that are available to be bound by the bridging unit. Such 4 + 2 nodes are predisposed to generate either discrete (0-D) supramolecular compounds (such as in this case) or (zigzag) 1-D chains. Co−NCS bond distances are 2.131(8) and 2.095(8) Å for Co−N1 and Co−N2′, respectively (Supporting Information, Table S4). The Pt(II) metal center is coordinated to two bridging SCN^- units (cis) and two nonbridging units (also cis), yielding the expected four-coordinate, square-planar geometry, but note that the four SCN^- units are not coplanar (as would be the case for the more ubiquitous CN^-); the cis-bridging pair is nearly coplanar with the PtS_4 plane, while the other two are 51° and 72° out of the plane (as defined by smallest cis-S−Pt−S−N torsion angle). The packing arrangement of **1** consists of tetranuclear units arranged in a 3-D environment via $\pi-\pi$ interactions of the 2,2′-bipyridine ligands.

The Cu(II)-containing version (**4**) is essentially isostructural with **1** (Supporting Information, Figure S1), except for the presence of the Jahn−Teller axis; the equatorial Cu−N bond lengths range between 2.002(5) and 2.077(6) Å, and the axial ones are between 2.361(6) and 2.217(5) Å (Supporting Information, Table S4).

dx.doi.org/10.1021/ic302360b | Inorg. Chem. 2013, 52, 4842−4852

Structural analysis of **6** revealed a double salt made of the $[Pt(SCN)_4]^{2-}$ anion and two $[Cu(bipy)(NCS)]^+$ cations (Figure 2). This complex is a decomposition product, indicative

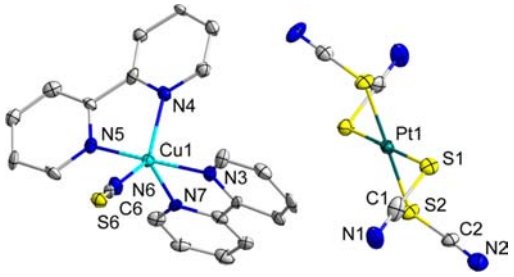

Figure 2. Structure of $[Cu(bipy)_2(NCS)]_2[Pt(SCN)_4]$ (**6**). Hydrogen atoms have been omitted for clarity. Thermal ellipsoids are drawn at 50% probability. Color code: light blue (Cu), green (Pt), blue (N), gray (C), yellow (S). Selected bond lengths (Å): Cu1–N3 = 1.991(7), Cu1–N4 = 2.066(7), Cu1–N5 = 1.981(7), Cu1–N7 = 2.115(7), Cu1–N6 = 1.996(8).

of some lability of the $[Pt(SCN)_4]^{2-}$ anion in water, transferring one SCN^- from the anion to the $[Cu(bipy)_2]^{2+}$ cation; the lower yield is also consistent with this picture. Its formation also suggests that the building block $[Pt(SCN)_4]^{2-}$ is more labile in a mixture of water and methanol compared to methanol only. Formation of **6** may also be assisted by its lower solubility in water. The four SCN^- units coordinated to the Pt(II) metal center are nonbridging, with two trans-SCN units nearly coplanar with the PtS_4 plane and the other two 75° out of the PtS_4 plane. The Cu(II) metal center is coordinated to two bipy ligands and the nonbridging SCN^- unit (Cu–NCS distance of 1.996(8) Å (Supporting Information, Table S4), leading to a five-coordinate distorted trigonal bipyramidal geometry, as defined by a τ value of 0.65.[79] No significant intermolecular contacts are present.

Synthesis and Structural Studies of $[M(en)_2Pt(XCN)_4]$ (X = S, M = Ni, Cu; X = Se, M = Cu). Addition of 2 equiv. of ethylenediamine (en) to a Cu(II) or Ni(II) salt followed by addition of a $[Pt(XCN)_4]^{2-}$ salt (X = S, Se) gave a series of related products of the form $[M(en)_2Pt(XCN)_4]$ (M = Cu, Ni). Initially, slow diffusion of $[Cu(en)_2](ClO_4)_2$ into a solution of $K_2[Pt(SCN)_4]$ in a Petri dish yielded only the cis complex *cis*-$[Cu(en)_2Pt(SCN)_4]$ (**7**). Changing the solvent composition or metal-to-ligand ratios did not result in crystallization of complexes other than **7**. However, layering the $K_2[Pt(SCN)_4]$ solution on top of the $[Cu(en)_2](ClO_4)_2$ resulted in crystallization of both brown **7** and purple **8**, both of which have the formula $[Cu(en)_2Pt(SCN)_4]$; representative crystals were manually separated. Using $Ni(NO_3)_2{\cdot}6H_2O$ instead, slow diffusion and layering of the two solutions generated the analogous $[Ni(en)_2Pt(SCN)_4]$ (**10**). By leaving a 1:1 mixture of $[Cu(en)_2](NO_3)_2$ and $(Bu_4N)_2[Pt(SeCN)_4]$ in a methanol/ethanol mixture overnight, the analogous $[Cu(en)_2Pt(SeCN)_4]$ system (**9**) crystallized out of the mother liquor as dark red/brown plates.

Structural studies revealed that **7** (Figure 3) forms a 1-D coordination polymer. The Cu(II) metal center is octahedral, with two bidentate en ligands in the equatorial plane (Cu–N bond lengths are between 2.007(3) and 2.028(3) Å; Supporting Information, Table S5) and two N-bound NCS- bridging units in the elongated axial positions (2.444(3) and 2.448(3) Å); this cation can be described as a trans 4 + 2 nodal site, which is

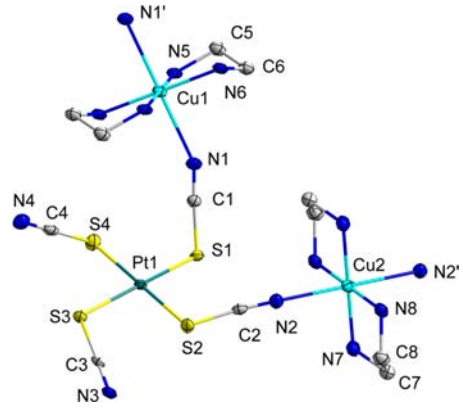

Figure 3. Molecular structure of *cis*-$[Cu(en)_2Pt(SCN)_4]$ (**7**). Hydrogen atoms have been omitted for clarity. Thermal ellipsoids are drawn at 50% probability. Color code: light blue (Cu), green (Pt), blue (N), gray (C), yellow (S). Selected bond lengths (Å): Cu1–N1 = 2.444(3), Cu1–N5 = 2.007(3), Cu1–N6 = 2.022(3), Cu2–N2 = 2.448(3), Cu2–N7 = 2.028(3), Cu2–N8 = 2.028(3).

likely to favor 1-D chain structures. Indeed, from the square-planar Pt(II) perspective, two cis SCN^- units bridge two Cu(II) centers, leading to a zigzag chain along the *ab* plane (Figure 4); all four SCN moieties are closer to coplanarity, with

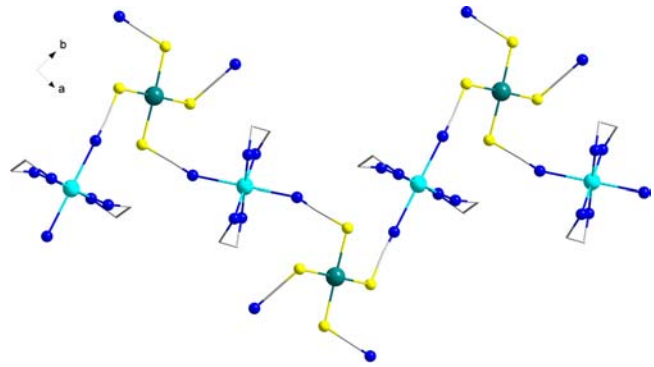

Figure 4. 1-D zigzag chain arrangement of *cis*-$[Cu(en)_2Pt(SCN)_4]$ (**7**). Hydrogen atoms have been omitted for clarity. Color code: light blue (Cu), green (Pt), blue (N), gray (C), yellow (S).

only one 35° out of the PtS_4 plane and the others within 15° or less. No significant intermolecular interactions between the chains were identified.

The structure of the Ni(II) complex **10** (Supporting Information, Figure S2) is analogous to that of **7**; two en ligands are equatorially coordinated, and two axial N-bound NCS bridges are present, with all Ni–N coordination distances around 2.095(3) Å (Supporting Information, Table S5). The supramolecular structure of **10** also consists of 1-D zigzag chains where two cis SCN^- units coordinated to the Pt(II) center bridge two $[Ni(en)_2]^{2+}$ species; the SCN^- moieties are tipped further out of the PtS_4 plane than in **7** (ranging from 0° to 63°).

Structural analysis (Figure 5) of the polymorphic purple crystals of $[Cu(en)_2Pt(SCN)_4]$ (**8**) confirmed that the components are identical to **7** but that the $[Pt(SCN)_4]^{2-}$ bridging unit is coordinated to the two Cu(II) centers using its trans SCN units (with a Cu–NCS distance of 2.504(2) Å; Supporting Information, Table S6) as opposed to the cis coordination of **7**. The bound Pt–SCN units are 81° out of the

dx.doi.org/10.1021/ic302360b | *Inorg. Chem.* 2013, 52, 4842–4852

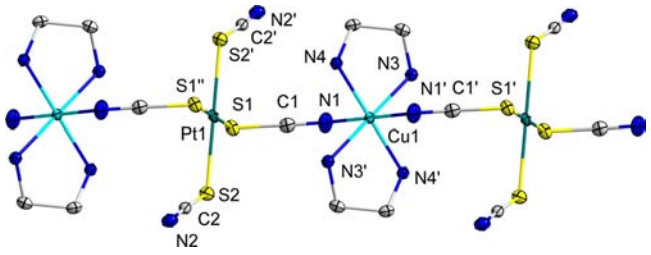

Figure 5. Linear 1-D chain structure of *trans*-$[Cu(en)_2Pt(SCN)_4]$ (**8**). Hydrogen atoms have been omitted for clarity. Thermal ellipsoids are drawn at 50% probability. Color code: light blue (Cu), green (Pt), blue (N), gray (C), yellow (S). Selected bond lengths (Å): Cu1−N1 = 2.504(2), Cu1−N4 = 2.019(2), Cu1−N3 = 2.014(2).

PtS_4 plane, while the unbound units are nearly coplanar (8° from the PtS_4 plane). This trans coordination of the $[Pt(SCN)_4]^{2-}$ combined with the trans 4 + 2 cation results in a linear chain of the repeating units, rather than the zigzag chain induced by the cis bridging in **7**. The fact that both **7** and **8** can be easily isolated from the same reaction mixture indicates that the two networks have very similar thermodynamic stabilities, as is commonly the case for such polymorphic supramolecular structures.[80−85] Note that no Ni(II)-containing version of **8** (i.e., with trans bridging $[Pt(SCN)_4]^{2-}$ units) could be isolated.

When the $[Pt(SeCN)_4]^{2-}$ unit is substituted for the SCN^- analogue in the synthesis with Cu(II) and en, a structure analogous to **8** is obtained; the two bridging $SeCN^-$ bridging units have a long Cu−N distance of 2.639(3) Å (Figure 6 and

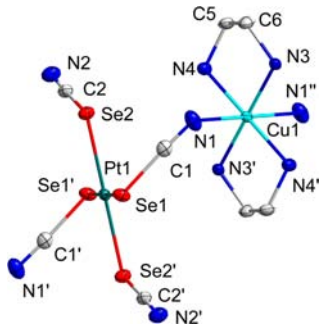

Figure 6. Molecular structure of *trans*-$[Cu(en)_2Pt(SeCN)_4]$ (**9**). Hydrogen atoms have been omitted for clarity. Thermal ellipsoids are drawn at 50% probability. Color code: light blue (Cu), green (Pt), blue (N), gray (C), red (Se). Selected bond lengths (Å): Cu1−N2 = 2.639(3), Cu1−N4 = 2.013(3), Cu1−N3 = 2.008(2), Se1−Se2′ = 3.7026(8).

Supporting Information, Table S6). The $[Pt(SeCN)_4]^{2-}$ unit is flatter than in **8**, with the bound and unbound Pt−SeCN units 56° and 4°, respectively, out of the PtS_4 plane (vs 81 and 8° for **8**). As in **8**, the trans coordination of the $[Pt(SeCN)_4]^{2-}$ units coupled with the trans 4 + 2 cation leads to formation of a similar 1-D linear chain. However, in this case Se−Se interchain interactions of 3.7026(8) Å link the chains together into a 2-D sheet (Figure 7). Such Se−Se interactions are common components of the supramolecular toolbox[86−88] (sum of the Se−Se van der Waals radii is 3.8 Å),[89] and this resulting increase in structural dimensionality suggests that further use of Se-containing building blocks is desirable.

Synthesis and Structural Studies of [M(terpy)Pt(SCN)$_4$] (M = Mn, Co) and [Mn(terpy)$_2$][Pt(SCN)$_4$]. Addition

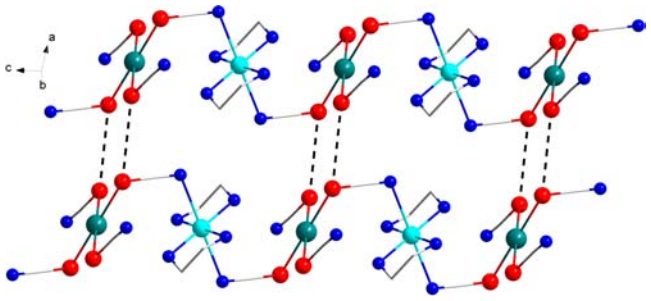

Figure 7. Supramolecular 2-D sheet arrangement of *trans*-$[Cu(en)_2Pt(SeCN)_4]$ (**9**). Hydrogen atoms have been omitted for clarity. Se−Se interactions are represented as the black fragmented bonds. Color code: light blue (Cu), green (Pt), blue (N), gray (C), red (Se).

of 1 equiv of 2,2′;6′,2″-terpyridine (terpy) to $MnCl_2·4H_2O$ in water followed by slow diffusion of this mixture into a solution of $K_2[Pt(SCN)_4]$ in methanol resulted in growth of crystals of the coordination polymer $[Mn(terpy)Pt(SCN)_4]$ (**11**). If mixed quickly or if the solvent mixture is altered, the double salt $[Mn(terpy)_2][Pt(SCN)_4]$ (**12**) was obtained instead. In the case of **13**, layering a 1:1 mixture of $Co(NO_3)_2·6H_2O$ and terpy in methanol over an aqueous solution of $K_2[Pt(SCN)_4]$ resulted in crystallization of both red plates and red blocks at the interface of the two solutions in a 65:35 ratio. Red plates were identified as $[Co(terpy)Pt(SCN)_4]$ (**13**) by X-ray crystallography and FT-IR, and red blocks were identified as $[Co(terpy)_2][Pt(SCN)_4]$ (**13b**) by FT-IR in comparison to **12**. The crystal structure of **13b** could not be obtained due to twinning and poor diffraction of the crystals. Individual elemental analyses of the complexes could not be obtained due to the difficulty of separating and purifying the cocrystallized complexes. Direct mixing of the reagents resulted in an amorphous powder for which IR and EA data was consistent with the data measured for the crystalline mixture of **13** and **13b**. Changing the method of crystallization, solvents, and ratios always resulted in a mixture of the two complexes.

Complex **11** (Figure 8) consists of a Mn(II) metal center octahedrally coordinated to one terpy ligand and three N-bound NCS^- units bridging to Pt(II) metal centers. Thus, the Mn(II) center can be termed a "3 + 3" nodal site using our classification lexicon described above: in this case, the metal

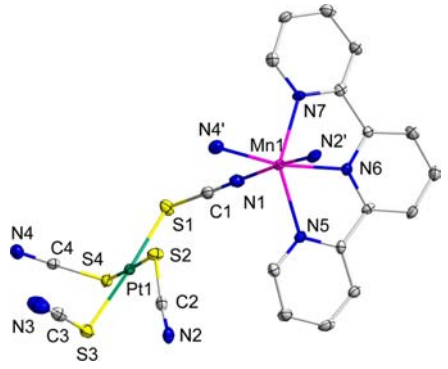

Figure 8. Molecular structure of $[Mn(terpy)Pt(SCN)_4]$ (**11**). Hydrogen atoms have been omitted for clarity. Thermal ellipsoids are drawn at 50% probability. Color code: purple (Mn), green (Pt), blue (N), gray (C), yellow (S). Selected bond lengths (Å): Mn1−N1 = 2.208(3), Mn1−N4′ = 2.180(3), Mn1−N6 = 2.221(3), Mn1−N2′ = 2.271(3), Mn1−N5 = 2.247(3), Mn1−N7 = 2.248(3).

dx.doi.org/10.1021/ic302360b | *Inorg. Chem.* 2013, 52, 4842−4852

center has three blocked coordination sites and three sites that are available to be bound by the bridging unit. It crystallizes in the monoclinic space group $P\ 2_1/n$. Mn−N distances for the tridentate terpy ligand range between 2.221(3) and 2.248(3) Å (Supporting Information, Table S7), as found in similar compounds.[90−95] Mn−NCS distances are 2.208(3), 2.271(3), and 2.180(3) Å (Supporting Information, Table S7). In the $[Pt(SCN)_4]$ unit, none of the four SCN^- moieties are coplanar with the PtS_4 plane; out-of-plane torsion angles range from 20° to 72°, with the nonbound unit 46° out of plane. This nonplanarity presumably is an important steric impediment to the formation of any Pt−Pt interactions in this system.

The supramolecular arrangement of **11** (Figure 9) consists of 2-D sheets in which one $[Mn(terpy)]^{2+}$ cation is coordinated to

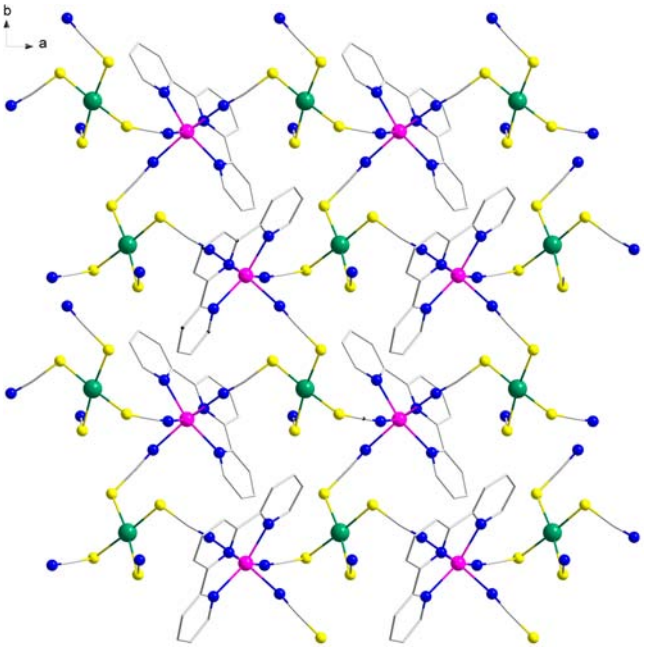

Figure 9. 2-D sheet arrangement of $[Mn(terpy)Pt(SCN)_4]$ (**11**). Hydrogen atoms have been omitted for clarity. Color code: purple (Mn), green (Pt), blue (N), gray (C), yellow (S).

three $[Pt(SCN)_4]^{2-}$ anions and each $[Pt(SCN)_4]^{2-}$ anion is coordinated to three distinct $[Mn(terpy)]^{2+}$ cations. A parallelogram of three Mn(terpy) and three $Pt(SCN)_4$ units can be inscribed; these supramolecular units are packed in a (6,3)-type grid array.[96,97] In **11**, the 3 + 3 node, which has more open coordination sites than the prior 4 + 2 nodes, are unsurprisingly inclined to generate systems with higher dimensionality (in this case 2-D). The sheets stack via $\pi-\pi$ interactions of the terpy ligands (not shown).

The structure of $[Co(terpy)Pt(SCN)_4]$ (**13**) is very similar to the Mn(II) analogue (Figure 10), except that the complex crystallizes in the orthorhombic group $Pna2_1$. As expected, the bond lengths of the ligands and the N-bound SCN^- units to the Co(II) metal center are slightly shorter. The supramolecular arrangement of **13** (Figure 11) is also similar to **11**, but the type of (6, 3) grid is slightly different. One noticeable structural difference that could be responsible for this change in symmetry is the orientation of the nonbridging SCN^- unit of the $[Pt(SCN)_4]^{2-}$ anion. In the case of **11**, the group is always oriented in the same direction along the *c* axis, whereas for **13** the orientation of the nonbridging group is alternating in the 2-

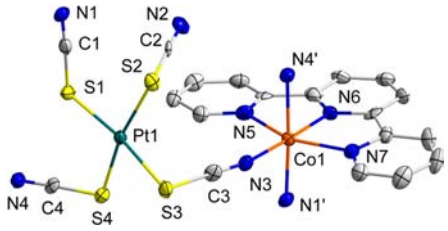

Figure 10. Molecular structure of $[Co(terpy)Pt(SCN)_4]$ (**13**). Hydrogen atoms have been omitted for clarity. Thermal ellipsoids are drawn at 50% probability. Color code: orange (Co), green (Pt), blue (N), gray (C), yellow (S). Selected bond lengths (Å): Co1−N1 = 2.330(4), Co1−N4″ = 1.956(4), Co1−N6 = 1.939(4), Co1−N3′ = 2.793(4), Co1−N5 = 2.037(4), Co1−N7 = 2.043(4).

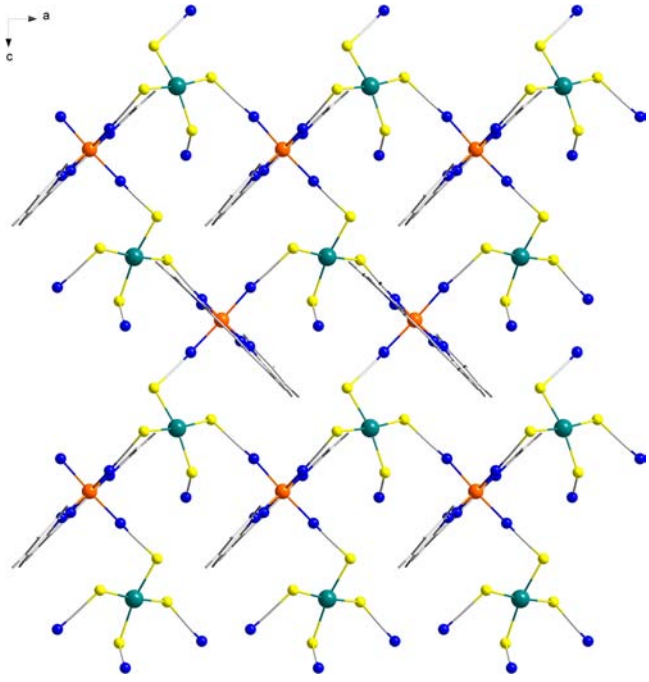

Figure 11. 2-D sheet arrangement of $[Co(terpy)Pt(SCN)_4]$ (**13**). Hydrogen atoms have been omitted for clarity. Color code: orange (Co), green (Pt), blue (N), gray (C), yellow (S).

D sheet. The PtS_4 out-of-plane angles for the SCN^- unit in **13** range from 17° to 70°, with the key unbound one being 61° (cf. 46° in **11**).

Complex **12** (Figure 12) is the double salt $[Mn(terpy)_2]$-$[Pt(SCN)_4]$ for which the Mn(II) metal center is coordinated to two 2,2′;6′,2″-terpyridine ligands and the $[Pt(SCN)_4]^{2-}$ unit is not coordinated to the Mn(II) metal center.

Synthesis and Structural Studies of [Cu(tmeda)Pt-(SCN)$_4$]. Addition of 1 equiv of $K_2[Pt(SCN)_4]$ to an aqueous solution of Cu(II) with 1 equiv of *N*,*N*,*N*′,*N*′-tetramethylethylenediamine (tmeda) yielded an immediate precipitate of $[Cu(tmeda)Pt(SCN)_4]$ (**14**). Slow diffusion of methanol solutions of the reagents in a Petri dish generated green crystals of **14** after several days.

The solid-state structure of **14** confirms the $[Cu(tmeda)Pt-(SCN)_4]$ formula, with one disordered (76:24) tmeda ligand bound to a five-coordinate Cu(II) center (Figure 13). The other three coordination sites contain bridging SCN^- units, leading to a distorted trigonal bipyramidal geometry; the Cu(II) center can thus be described as a "2 + 3" nodal site. The Cu−N(tmeda) distances are 2.044(5) and 2.047(5) Å

dx.doi.org/10.1021/ic302360b | *Inorg. Chem.* 2013, 52, 4842−4852

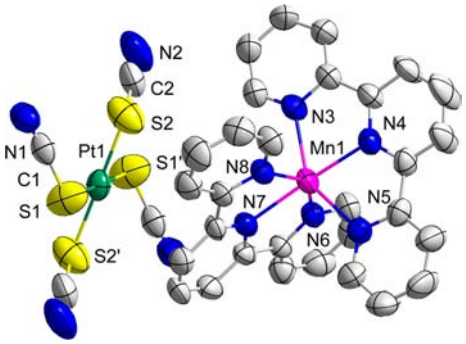

Figure 12. Molecular structure of $[Mn(terpy)_2][Pt(SCN)_4]$ (**12**). Hydrogen atoms have been omitted for clarity. Thermal ellipsoids are drawn at 50% probability. Color code: purple (Mn), green (Pt), blue (N), gray (C), yellow (S). Selected bond lengths (Å): Mn1−N3 = 2.239(6), Mn1−N4 = 2.198(5), Mn1−N5 = 2.262(5), Mn1−N6 = 2.234(5), Mn1−N7 = 2.195(5), Mn1−N8 = 2.246(5).

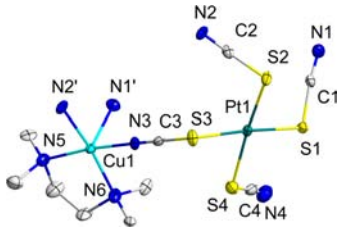

Figure 13. Molecular structure of $[Cu(tmeda)Pt(SCN)_4]$ (**14**). Hydrogen atoms have been omitted for clarity. Thermal ellipsoids are drawn at 50% probability. Color code: light blue (Cu), green (Pt), blue (N), gray (C), yellow (S). Selected bond lengths (Å): Cu1−N1′ = 2.287(6), Cu1−N3 = 1.978(6), Cu1−N2′ = 2.002(7), Cu1−N5 = 2.047(10), Cu1−N6 = 2.070(9).

(Supporting Information, Table S8). Cu−NCS distances are 2.288(6), 1.994(7), and 1.976(6) Å for N1, N2′, and N3″, respectively. The SCN units tilt out of the PtS_4 plane by 27−58°.

This leads to a supramolecular arrangement of wavy 2-D sheets along the *ab* plane in which only one SCN unit of the $[Pt(SCN)_4]^{2-}$ remains uncoordinated (Figure 14); the dimensionality of the polymer generated by this "2 + 3" node is analogous to that of the "3 + 3" node present in **6** and **7**. The unbound SCN^- unit is aligned toward the sixth Cu(II) coordination site, with a Cu−N4 distance of 2.94 Å; this is too far to be considered a significant metal−ligand interaction, although it could shorten substantially at lower temperatures.

Synthesis and Structural Studies of $[Pb(phen)_2Pt(SCN)_4]$. Addition of 2 equiv of 1,10-phenanthroline (phen) to 1 equiv of $Pb(ClO_4)_2{\cdot}6H_2O$ followed by addition of 1 equiv of $K_2[Pt(SCN)_4]$ (all in water/methanol) resulted in a powder mixture composed of $[Pb(phen)_2Pt(SCN)_4]$ (**15**) as a minor product and an unknown polymorph of **15** as a major product as revealed by PXRD (Supporting Information, Figure S8). The two polymorphs could not be separated from the powdered mixture. However, single crystals of **15** were obtained from a cooled aqueous/methanol solution of $[Pb(phen)_2](NO_3)_2$ and $K_2[Pt(SCN)_4]$. Further studies are underway to analyze the structural, optical, and thermal properties of the unidentified polymorph.

In the solid-state structure, the Pb(II) ion is coordinated to two phen ligands and four SCN units, resulting in an 8-coordinate geometry (Figure 15). The phen ligands are

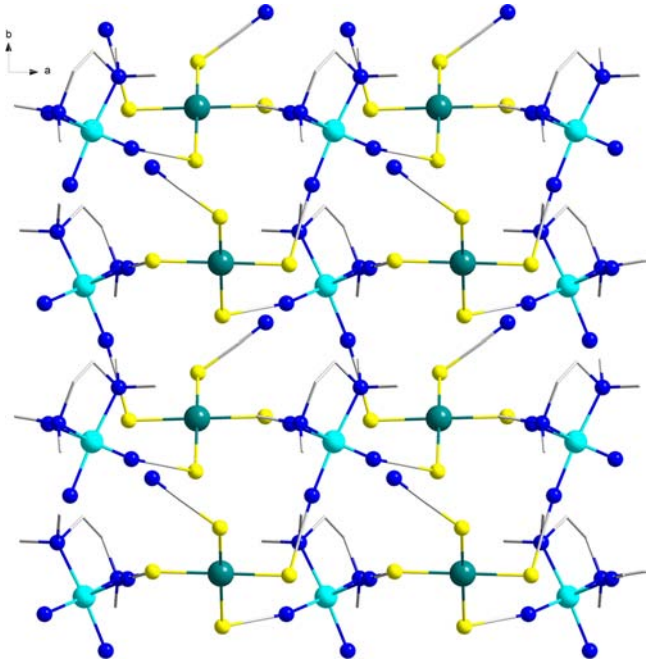

Figure 14. 2-D sheet arrangement of $[Cu(tmeda)Pt(SCN)_4]$ (**14**). Hydrogen atoms have been omitted for clarity. Color code: light blue (Cu), green (Pt), blue (N), gray (C), yellow (S).

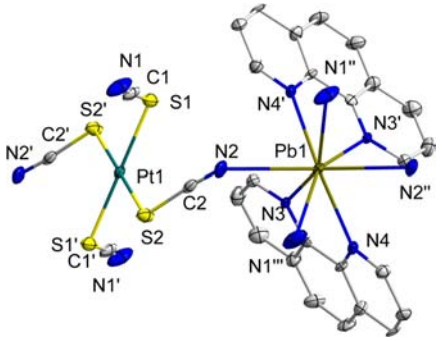

Figure 15. Molecular structure of $[Pb(phen)_2Pt(SCN)_4]$ (**15**). Hydrogen atoms have been omitted for clarity. Thermal ellipsoids are drawn at 50% probability. Color code: dark yellow (Pb), green (Pt), blue (N), gray (C), yellow (S). Selected bond lengths (Å): Pb1−N1′ = 2.996(8). Pb1−N3 = 2.608(6), Pb1−N2 = 2.811(6), Pb1−N4 = 2.575(6).

coordinated to the Pb(II) in a cis geometry but in a more parallel alignment compared to **1**. The coordination distances to the Pb(II) ion of the SCN^- units are 2.811(6) and 2.996(8) Å for Pb−N2 and Pb−N1, respectively (Supporting Information, Table S9); this difference is reflective of the stereochemically active lone pair on the Pb(II) ion. A similar coordination sphere and bond length range was observed in the related $[Pb(phen)_2][Au(CN)_2]_2$[98] and can be described as a "4 + 4" connecting node. Along the *a* axis, the SCN^- units with the shorter coordination distances form a 1-D chain. The two SCN^- units with longer coordination distances connect two adjacent 1-D chains, effectively rendering this system a 3-D coordination polymer.

Looking down the *c* axis, **15** appears to contain channels lined by phen ligands (Figure 16), but attempts to measure the N_2-adsorption properties of the material were unsuccessful.

dx.doi.org/10.1021/ic302360b | *Inorg. Chem.* 2013, 52, 4842−4852

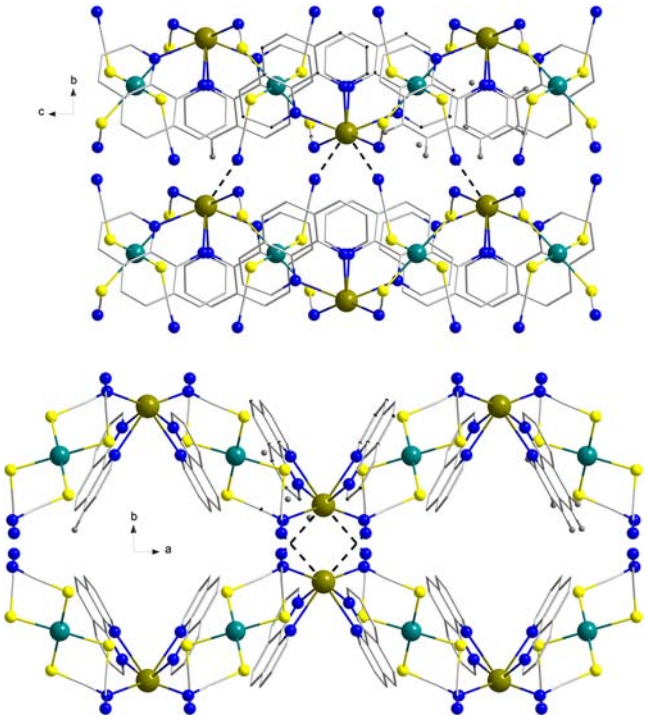

Figure 16. 3-D supramolecular arrangement of $[Pb(phen)_2Pt(SCN)_4]$ (**15**) viewed down the *a* axis (top) and down the *c* axis (bottom). Hydrogen atoms have been omitted for clarity. Interchain coordination is depicted as black dashed lines. Color code: dark yellow (Pb), green (Pt), blue (N), gray (C), yellow (S).

Magnetic Properties. Direct current susceptibility measurements were performed for selected paramagnetic compounds between 1.8 and 300 K at 1000 Oe. In all cases, the $\chi_M T$ vs T product at room temperature is close to the value for noninteracting ions. As the temperature goes down, a slow decrease in $\chi_M T$ is observed, which might be due to intermolecular antiferromagnetic interactions, magnetic anisotropy, and/or thermal depopulation of the low-lying excited states, depending on the compound. In general, the paramagnetic transition metal centers in the complexes are well separated both through bonds and through space, and thus, given that all interactions were weak at best, no further analysis was conducted for the compounds.

DISCUSSION

With this substantial set of $[Pt(SCN)_4]$-based systems in hand, in an effort to comprehend the supramolecular arrangement favored in each of the complexes, the structures were examined by considering the effects of (a) the transition metal used, (b) the effective coordination sphere of the transition metals (i.e., the capping ligand employed), and (c) the bridging propensity of the $[Pt(SCN)_4]^{2-}$ unit, which can bridge up to four transition metal ions.

Influence of the Transition Metal Ion/Ancillary Ligand Combination. In most cases, the coordination polymers herein were synthesized using first-row transition metals, which usually possess between four and six coordination sites. When increasing the amount of available coordination sites using the very large Pb(II) center, eight coordination sites became available; obviously, all else being equal, a larger number of open coordination sites on the metal cation are likely to lead to a greater dimensionality in the resulting coordination polymer.

That said, the capping ligands play a more definitive role in directing the supramolecular arrangement of the system. In most of the complexes reported herein, the capping ligand was likely the determining factor of the resulting architecture as it controlled the number of available coordination sites on the transition metal center. As such, both the en and the bipy ligands cap four of the six coordination sites of the cations, leading to coordination of two SCN^- units to the metal center. However, two en ligands coordinated in a trans fashion, leading to formation of a 1-D coordination polymer as opposed to a molecular tetranuclear complex for the two cis-bound bipy ligands. In the case of terpy, leaving three open coordination sites (on octahedral metal centers) effectively resulted in a 2-D coordination polymer, while in the case of tmeda, only one unit binds for steric reasons, leaving space for three to four SCN^- units, generating a 2-D coordination polymer as well.

Thus, using our crude classification scheme X + Y with respect to metal nodes, where X represents the number of coordination sites occupied by the ligand and Y is the number of remaining sites on the cation, a 4 + 2 node generates either a molecular tetranuclear complex (**1**, **4**) or a 1-D coordination polymer (**7**−**10**), depending on whether the two open sites are in a cis or trans orientation. The 3 + 3 (**11**, **13**) and 2 + 3 (**14**) nodes resulted in 2-D sheet structures, and the 4 + 4 (**15**) node resulted in a 3-D array. Thus, as mentioned above, the highest amount of remaining open coordination sites (Y) favors an increased dimensionality in the supramolecular arrangement of the polymers.

Influence of the coordination of $[Pt(SCN)_4]^{2-}$. The $[Pt(SCN)_4]^{2-}$ building block can coordinate up to four different metal cations via the SCN^- bridging moieties. For example, in **6**, the unit does not coordinate to any transition metal. In some cases, two cations are bridged using either cis (**1**, **4**, **7**, **10**) or trans (**8**, **9**) coordination of two SCN^- units. In **11**, **13**, and **14**, three of the four SCN^- moieties are bridged to the cations. Finally, in **15**, all four of the SCN^- units bridge to Pb(II) cations, generating intra- or interchain connections. Clearly, a larger number of metal centers bridged by the $[Pt(SCN)_4]^{2-}$ unit will result in greater dimensionality in the resulting product. However, control over the number and geometry of the bridging SCN^- units was not achievable by changing the reaction conditions of the syntheses.

In addition, the fact that the $[Pt(SCN)_4]^{2-}$ building block is not strictly planar as opposed to the $[Pt(CN)_4]^{2-}$ analogue generates further degrees of freedom in structure determination. In the systems presented herein, the Pt−S−C−N torsion angles (i.e., the amount that each SCN group lies out of the PtS_4 plane) vary greatly depending on multiple factors, including the number of metal cations the $[Pt(SCN)_4]^{2-}$ building block is connected to and also steric and hydrogen-bonding interactions between the ancillary capping ligands on the metal cation and the dangling SCN^- species. This structural aspect may be controllable by judicious choice of ancillary ligand, but in the series of complexes presented herein, it is very difficult to isolate the factors that favor one spatial arrangement of SCN^- units over another.

In terms of the Se analogue $[Pt(SeCN)_4]^{2-}$, **9** appears to represent the first reported coordination polymer with this building block; it showed increased dimensionality via Se−Se van der Waals interactions with its adjacent neighbor compared to the S analogue (**8**). This suggests that incorporation of Se vs S in these coordination polymers has the potential to increase

dx.doi.org/10.1021/ic302360b | *Inorg. Chem.* 2013, 52, 4842−4852

the amount of intermolecular interactions and thus the dimensionality of the resulting architecture.

On a more general note, when compared to similar structures synthesized using d^8 square-planar $[Au(CN)_4]^-$ instead of $[Pt(XCN)_4]^{2-}$ (X = S, Se), no interactions were denoted between the Pt(II) centers and any other donors (e.g., adjacent $^-$NCS units), as opposed to the readily observed apical/axial Au(III)−NC interactions between the Au(III) centers and the N(cyano) units from adjacent $[Au(CN)_4]^-$ moieties.[73,99−103] Importantly, compared to the d^8 $[Pt(CN)_4]^{2-}$ unit, no Pt−Pt metallophilic interactions were observed in any of these systems, which is somewhat surprising given the fact that soft ligands such as S and Se donors tend to favor such metallophilic interactions in d^{10} Au-based systems. It is possible that the nonplanarity of the $[Pt(XCN)_4]^{2-}$ units may restrict their ability to form such metal-based attractive interactions.

CONCLUSION

The first coordination polymers using the $[Pt(XCN)_4]^{2-}$ (X = S, Se) building block have been synthesized and structurally characterized, illustrating their use as viable building blocks; materials with dimensionalities from zero to three were prepared, depending on the metal cation and ancillary capping ligand employed. Although the overall dimensionality could be tuned in a rational fashion, the nonplanarity of these square-planar dianions compared to the $[Pt(CN)_4]^{2-}$ analogue renders a fine level of structural control more challenging and also likely helps to block formation of any metallophilic interactions. The Se analogue exhibited additional intermolecular Se---Se interactions, indicating that further exploration of this and related building blocks would be worthwhile.

ASSOCIATED CONTENT

Supporting Information

Crystallographic data and bond lengths/angle tables for **1**, **4**, and **6**−**15**, and powder X-ray diffraction data for **1**, **2**, **7**, **10**, **12**, **14**, and **15**; complete crystallographic data in CIF format for all reported crystal structures. This material is available free of charge via the Internet at http://pubs.acs.org.

AUTHOR INFORMATION

Corresponding Author

*Phone: 1-778-782-4887 (D.B.L.); 81-92-642-2596 (K.S.). Fax: 1-778-782-3765 (D.B.L.). E-mail: dleznoff@sfu.ca (D.B.L.); ksakai@chem.kyushu-univ.jp (K.S.).

Notes

The authors declare no competing financial interest.

ACKNOWLEDGMENTS

Financial support from NSERC, SFU, and Natural Resources of Canada (ARG) is gratefully acknowledged. The present work was also supported by a Grant-in-Aid for the Global COE Program, "Science for Future Molecular Systems", from the Ministry of Education, Culture, Science, Sports and Technology of Japan, a Grant-in-Aid for Scientific Research (A) (No. 17205008), a Grant-in-Aid for Scientific Research on Priority Areas (No. 16074216 of 434: "Chemistry of Coordination Space"), and a Grant-in-Aid for Specially Promoted Research (No. 18002016) from the Ministry of Education, Culture, Sports, Science, and Technology of Japan. M.K. acknowledges Research Fellowships of the Japan Society for the Promotion of Science for Young Scientist. D.B.L. is grateful to JSPS for a Long-term Invitation Fellowship.

REFERENCES

(1) Moulton, B.; Zaworotko, M. J. *Chem. Rev.* **2001**, *101*, 1629.
(2) Eddaoudi, M.; Moler, D. B.; Li, H. L.; Chen, B. L.; Reineke, T. M.; O'Keeffe, M.; Yaghi, O. M. *Acc. Chem. Res.* **2001**, *34*, 319.
(3) Holliday, B. J.; Mirkin, C. A. *Angew. Chem., Int. Ed.* **2001**, *40*, 2022.
(4) Leong, W. L.; Vittal, J. J. *Chem. Rev.* **2011**, *111*, 688.
(5) Batten, S. R.; Neville, S. M.; Turner, D. R. *Coordination Polymers: Design, Analysis and Application*; Royal Society of Chemistry: Cambridge, 2009.
(6) Wang, S.; Huang, W. *Coord. Chem. Rev.* **2012**, *256*, 439.
(7) Katz, M. J.; Sakai, K.; Leznoff, D. B. *Chem. Soc. Rev.* **2008**, *37*, 1884.
(8) Braga, D.; Grepioni, F. *Making crystals by design: methods, techniques and applications*; Wiley-VCH: Weinheim, 2007.
(9) Ciurtin, D. M.; Smith, M. D.; zur Loye, H. C. *J. Chem. Soc., Dalton Trans.* **2003**, 1245.
(10) Hoskins, B. F.; Robson, R. *J. Am. Chem. Soc.* **1990**, *112*, 1546.
(11) Gardner, G. B.; Venkataraman, D.; Moore, J. S.; Lee, S. *Nature* **1995**, *374*, 792.
(12) Keller, S. W. *Angew. Chem., Int. Ed.* **1997**, *36*, 247.
(13) Orr, G. W.; Barbour, L. J.; Atwood, J. L. *Science* **1999**, *285*, 1049.
(14) Yaghi, O. M.; Li, H. L.; Davis, C.; Richardson, D.; Groy, T. L. *Acc. Chem. Res.* **1998**, *31*, 474.
(15) Chesnut, D. J.; Hagrman, D.; Zapf, P. J.; Hammond, R. P.; LaDuca, R.; Haushalter, R. C.; Zubieta, J. *Coord. Chem. Rev.* **1999**, *192*, 737.
(16) Hagrman, P. J.; Finn, R. C.; Zubieta, J. *Solid State Sci.* **2001**, *3*, 745.
(17) Stock, N.; Biswas, S. *Chem. Rev.* **2012**, *112*, 933.
(18) Sato, O.; Lyoda, T.; Fujishima, A.; Hashimoto, K. *Science* **1996**, *272*, 704.
(19) Verdaguer, M.; Bleuzen, A.; Marvaud, V.; Vaissermann, J.; Seuleiman, M.; Desplanches, C.; Scuiller, A.; Train, C.; Garde, R.; Gelly, G.; Lomenech, C.; Rosenman, I.; Veillet, P.; Cartier, C.; Villain, F. *Coord. Chem. Rev.* **1999**, *190−192*, 1023.
(20) Lind, C. *Materials* **2012**, *5*, 1125.
(21) Vaucher, S.; Fielden, J.; Li, M.; Dujardin, E.; Mann, S. *Nano Lett.* **2002**, *2*, 225.
(22) Zhou, P. H.; Xue, D. S.; Luo, H. Q.; Chen, X. G. *Nano Lett.* **2002**, *2*, 845.
(23) Uemura, T.; Kitagawa, S. *J. Am. Chem. Soc.* **2003**, *125*, 7814.
(24) Dunbar, K. R.; Heintz, R. A. *Prog. Inorg. Chem.* **1997**, *45*, 283.
(25) Ohba, M.; Okawa, H. *Coord. Chem. Rev.* **2000**, *198*, 313.
(26) Cernak, J.; Orendac, M.; Potocnak, I.; Chomic, J.; Orendacova, A.; Skorsepa, J.; Feher, A. *Coord. Chem. Rev.* **2005**, *224*, 51.
(27) Tanase, S.; Reedijk, J. *Coord. Chem. Rev.* **2006**, *250*, 2501.
(28) Shatruk, M.; Avendano, C.; Dunbar, K. R. *Prog. Inorg. Chem.* **2009**, *56*, 155.
(29) Lefebvre, J.; Leznoff, D. B. In *Metal and Metalloid-Containing Polymers*; Abd-El-Aziz, A. S., Carraher, C. E., Jr.; Pittman, C. U., Jr.; Zeldin, M., Eds.; Wiley: New York, 2005; Vol. *5*, p 155.
(30) Nishikiori, S.; Iwamoto, T. *Bull. Chem. Soc. Jpn.* **1983**, *56*, 3246.
(31) Kajnakova, M.; Cernak, J.; Kavecansky, V.; Gerard, F.; Papageorgiou, T.; Orendac, M.; Orendacova, A.; Feher, A. *Solid State Sci.* **2006**, *8*, 203.
(32) Shaikh, N.; Panja, A.; Goswami, S.; Banerjee, P.; Kubiak, M.; Ciunik, Z.; Puchalska, M.; Legendziewicz, J. *Indian J. Chem.* **2004**, *43*, 1403.
(33) Kendi, E.; Ulku, D. *Z. Kristallogr.* **1976**, *144*, 91.
(34) Nishikiori, S.-I.; Iwamoto, T. *Inorg. Chem.* **1986**, *25*, 788.
(35) Miyoshi, T.; Iwamoto, T.; Sasaki, Y. *Inorg. Chim. Acta* **1972**, *6*, 59.
(36) Lu, R.; Zhou, H.; Chen, Y.; Xiao, J.; Yuan, A. *J. Coord. Chem.* **2010**, *63*, 794.

(37) Ding, E.; Sturgeon, M. R.; Rath, A.; Chen, X.; Keane, M. A.; Shore, S. G. *Inorg. Chem.* **2009**, *48*, 325.
(38) Geisheimer, A. R.; Huang, W.; Pacradouni, V.; Sabok-Sayr, S. A.; Sonier, J. E.; Leznoff, D. B. *Dalton Trans.* **2011**, *40*, 7505.
(39) Martínez, V.; Gaspar, A. B.; Muñoz, M. C.; Bukin, G. V.; Levchenko, G.; Real, J. A. *Chem.—Eur. J.* **2009**, *15*, 10960.
(40) Needham, G. F.; Johnson, P. L.; Williams, J. M. *Acta Cryst.* **1977**, *B33*, 1581.
(41) Dillinger, R.; Gliemann, G.; Pfleger, H. P.; Krogmann, K. *Inorg. Chem.* **1983**, *22*, 1366.
(42) Akhmedov, A. I.; Yanovsky, A. I.; Babkov, A. V.; Struchkov, Y. T. *Coord. Khim. (Russ.)* **1983**, *9*, 1138.
(43) Brozik, J. A.; Scott, B. L.; Swanson, B. I. *Inorg. Chim. Acta* **1999**, *294*, 275.
(44) Krogmann, K.; Keim, A.; Stahl, R.; Pfleger, H. P. *Mol. Cryst. Liq. Cryst.* **1985**, *120*, 401.
(45) Potocnak, I.; Vavra, M.; Cizmar, E.; Tibenska, K.; Orendacova, A.; Steinborn, D.; Wagner, C.; Dusek, M.; Fejfarova, K.; Schmidt, H.; Muller, T.; Orendac, M.; Feher, A. *J. Solid State Chem.* **2006**, *179*, 1965.
(46) Liu, F.; Chen, W. *J. Coord. Chem.* **2006**, *59*, 1629.
(47) Schollhorn, H.; Thewalt, U.; Raudaschl-Sieber, G.; Lippert, B. *Inorg. Chim. Acta* **1986**, *124*, 207.
(48) Flay, M.-L.; Vahrenkamp, H. *Eur. J. Inorg. Chem.* **2003**, 1719.
(49) Olmstead, M. M.; Lee, M. A.; Stork, J. R. *Acta Crystallogr., Sect. E* **2005**, *61*, m1048.
(50) Cordiner, R. L.; Feroze, M. P.; Lledo-Fernandez, C.; Albesa-Jove, D.; Howard, J. A. K.; Low, P. J. *Inorg. Chim. Acta* **2006**, *359*, 3459.
(51) Dechambenoit, P.; Ferlay, S.; Hosseini, M. W.; Kyritsakas, N. *Chem. Commun.* **2007**, 4626.
(52) Vavra, M.; Potocnak, I.; Kajnakova, M.; Cizmar, E.; Feher, A. *Inorg. Chem. Commun.* **2009**, *12*, 396.
(53) Falvello, L. R.; Tomas, M. *Chem. Commun.* **1999**, 273.
(54) Potocnak, I.; Vavra, M.; Cizmar, E.; Kajnakova, M.; Radvakova, A.; Steinborn, D.; Zvyagin, S. A.; Wosnitza, J.; Feher, A. *J. Solid State Chem.* **2009**, *182*, 196.
(55) Jana, A. D.; Saha, R.; Ghosh, A. K.; Manna, S.; Ribas, J.; Chaudhuri, N. R.; Mostafa, G. *Polyhedron* **2009**, *28*, 3065.
(56) Potocnak, I.; Vavra, M.; Cizmar, E.; Dusek, M.; Muller, T.; Steinborn, D. *Inorg. Chim. Acta* **2009**, *362*, 4152.
(57) Stojanovic, M.; Robinson, N. J.; Chen, X.; Sykora, R. E. *Inorg. Chim. Acta* **2011**, *370*, 513.
(58) Doerrer, L. H. *Comments Inorg. Chem.* **2008**, *29*, 93.
(59) Buss, C. E.; Anderson, C. E.; Pomije, M. K.; Lutz, C. M.; Britton, D.; Mann, K. R. *J. Am. Chem. Soc.* **1998**, *120*, 7783.
(60) Katz, M. J.; Sakai, K.; Leznoff, D. B. *Chem. Soc. Rev.* **2008**, *37*, 1884.
(61) Levasseur-Theriault, G.; Reber, C.; Aronica, C.; Luneau, D. *Inorg. Chem.* **2006**, *45*, 2379.
(62) Gysling, H. J.; Luss, H. R. *Organometallics* **1984**, *3*, 596.
(63) Dou, J.-M.; Liu, Y.; Sun, D.-Z.; Li, X.; Zheng, P.-J.; Du, C.-X.; Zhu, Y. *Huaxue Xuebao (Chin.) (Acta Chim. Sinica)* **2001**, *59*, 918.
(64) Zhu, D.-Z.; Song, X.-M.; Dou, J.-M.; Liu, Y.; Wang, D.-Q.; Yong, W.; Zheng, P.-J. *Wuji Huaxue Xuebao (Chin.) (Chin. J. Inorg. Chem.)* **2002**, *18*, 697.
(65) Li, Z.-X.; Zhang, Z.-H.; Wang, T.; Li, D.-C.; Wang, D.-Q.; Dou, J.-M.; Zheng, P.-J. *Huaxue Xuebao (Chin.) (Acta Chim. Sinica)* **2002**, *60*, 1465.
(66) Dou, J.; Gao, X.; Dong, F.; Li, D.; Wang, D. *Dalton Trans.* **2004**, 2918.
(67) Niu, M.-J.; Wang, D.-Q.; Li, D.-C.; Dou, J.-M. *Z. Kristallogr.* **2005**, *220*, 188.
(68) Liu, Y.; Dou, J.; Zhu, L.; Sun, D.; Zheng, P. *Indian J. Chem.* **2000**, *39*, 983.
(69) Ha, K. *Acta Crystallogr., Sect. E* **2010**, *66*, m200.
(70) Konno, M.; Ohfuchi, K.; Shirotani, I.; Yamochi, H.; Saito, G. *Z. Kristallogr.* **1997**, *212*, 121.
(71) Rhode, J.-U.; von Malottki, B.; Preetz, W. Z. *Anorg. Allg. Chem.* **2000**, *626*, 905.
(72) Crawford, P. C.; Gillon, A. L.; Green, J.; Orpen, A. G.; Podesta, T. J.; Pritchard, S. V. *Cryst. Eng. Commun.* **2004**, *6*, 419.
(73) Aoki, K.; Hu, N.-H.; Tokuno, T.; Adeyemo, A. O.; Williams, G. N. *Inorg. Chim. Acta* **1999**, *290*, 145.
(74) Burmeister, J. L.; Williams, L. E. *Inorg. Chem.* **1996**, *5*, 1113.
(75) Kahn, O. *Molecular Magnetism*; VCH: Weinheim, 1993.
(76) *Chemistry experiments*, 4th ed.; The Chemical Society of Japan; Vol. *17*, p 162.
(77) Sakai, K.; Miyabe, Y. *Acta Crystallogr.* **2004**, *C60*, m69.
(78) Dunbar, K. R.; Heintz, R. A. *Prog. Inorg. Chem.* **1997**, *45*, 283.
(79) Addison, A. W.; Rao, T. N. *J. Chem. Soc., Dalton Trans.* **1984**, 1349.
(80) Boeckmann, J.; Evers, N.; Näther, C. *Cryst. Eng. Commun.* **2012**, *14*, 1094.
(81) Zhang, J. P.; Huang, X. C.; Chen, X. M. *Chem. Soc. Rev.* **2009**, *38*, 2385.
(82) Masaoka, S.; Tanaka, D.; Nakanishi, Y.; Kitagawa, S. *Angew. Chem., Int. Ed.* **2004**, *43*, 2530.
(83) Chen, C. L.; Yu, Z. Q.; Zhang, Q.; Pan, M.; Zhang, J. Y.; Zhao, C. Y.; Su, C. Y. *Cryst. Growth Des.* **2008**, *8*, 897.
(84) Monge, A.; Gándara, F.; Gutiérrez-Puebla, E.; Snejko, N. *Cryst. Eng. Commun.* **2011**, *13*, 5031.
(85) Bernstein, J. *Polymorphism in Molecular Crystals*; Oxford University Press: Oxford, 2002.
(86) Karjalainen, M. M.; Laitinen, R. S. *Inorg. Chim. Acta* **2012**, *390*, 79.
(87) Bleiholder, C.; Werz, D. B.; Köppel, H.; Gleiter, R. *J. Am. Chem. Soc.* **2006**, *128*, 2666.
(88) Mundt, O.; Becker, G.; Baumgarten, J.; Riffel, H.; Simon, A. *Z. Anorg. Allg. Chem.* **2006**, *632*, 1687.
(89) Bondi, A. *J. Phys. Chem.* **1964**, *68*, 441.
(90) Rompel, A.; Bond, A. D.; McKenzie, C. J. *Acta Crystallogr., Sect. E* **2004**, *60*, m1759.
(91) Freire, E.; Baggio, S.; Garland, M. T.; Baggio, R. *Acta Crystallogr., C* **2001**, *57*, 1403.
(92) Bhula, R.; Weatherburn, D. C. *Aust. J. Chem.* **1991**, *44*, 303.
(93) Baffert, C.; Romero, I.; Pecaut, J.; Llobet, A.; Deronzier, A.; Collomb, M.-N. *Inorg. Chim. Acta* **2004**, *357*, 3430.
(94) Oshio, H.; Spiering, H.; Ksenofontov, V.; Renz, F.; Gutlich, P. *Inorg. Chem.* **2001**, *40*, 1143.
(95) Geisheimer, A. R.; Wren, J. E. C.; Michaelis, V. K.; Kobayashi, M.; Sakai, K.; Kroeker, S.; Leznoff, D. B. *Inorg. Chem.* **2011**, *50*, 1265.
(96) Batten, S. R.; Robson, R. *Angew. Chem., Int. Ed.* **1998**, *37*, 1460.
(97) Öhrström, L.; Larsson, K. *Molecule-Based Materials: The Structural Network Approach*; Elsevier: Amsterdam, 2005.
(98) Katz, M. J.; Michaelis, V. K.; Aguiar, P. M.; Yson, R.; Lu, H.; Kaluarachchi, H.; Batchelor, R. J.; Schreckenbach, G.; Kroeker, S.; Patterson, H. H.; Leznoff, D. B. *Inorg. Chem.* **2008**, *47*, 6353.
(99) Shorrock, C. J.; Jong, H.; Batchelor, R. J.; Leznoff, D. B. *Inorg. Chem.* **2003**, *42*, 3917.
(100) Katz, M. J.; Shorrock, C. J.; Batchelor, R. J.; Leznoff, D. B. *Inorg. Chem.* **2006**, *45*, 1757.
(101) Katz, M. J.; Kaluarachchi, H.; Batchelor, R. J.; Schatte, G.; Leznoff, D. B. *Cryst. Growth Des.* **2007**, *7*, 1946.
(102) Vitoria, P.; Muga, I.; Gutierrez-Zorrilla, J. M.; Luque, A.; Roman, P.; Lezama, L.; Zuniga, F. J.; Beitia, J. I. *Inorg. Chem.* **2003**, *42*, 960.
(103) Leznoff, D. B.; Shorrock, C. J.; Batchelor, R. J. *Gold Bull.* **2007**, *40*, 36.
(104) Sheldrick, G. M. *SHELXL-97, Program for the Solution of Crystal Structures*; University of Göttingen: Göttingen, Germany, 1997.